

 Open access • Journal Article • DOI:10.1021/ES403466P

Fate of ZnO nanoparticles in soils and cowpea (*Vigna unguiculata*). — [Source link](#)

[Peng Wang](#), [Neal W. Menzies](#), [Enzo Lombi](#), [Brigid A. McKenna](#) ...+4 more authors





Institutions: [University of Queensland](#), [University of South Australia](#), [Australian Synchrotron](#)

Published on: 14 Nov 2013 - [Environmental Science & Technology](#) (American Chemical Society)

Topics: [Soil chemistry](#) and [Vigna](#)

Related papers:

- [Soybean susceptibility to manufactured nanomaterials with evidence for food quality and soil fertility interruption.](#)
- [Root uptake and phytotoxicity of ZnO nanoparticles.](#)
- [CuO and ZnO nanoparticles: phytotoxicity, metal speciation, and induction of oxidative stress in sand-grown wheat](#)
- [In situ synchrotron X-ray fluorescence mapping and speciation of CeO₂ and ZnO nanoparticles in soil cultivated soybean \(*Glycine max*\).](#)
- [Fate of CuO and ZnO nano- and microparticles in the plant environment.](#)

Share this paper:    

View more about this paper here: <https://typeset.io/papers/fate-of-zno-nanoparticles-in-soils-and-cowpea-vigna-x2ow82isid>

This document is confidential and is proprietary to the American Chemical Society and its authors. Do not copy or disclose without written permission. If you have received this item in error, notify the sender and delete all copies.

Fate of ZnO nanoparticles in soils and cowpea (*Vigna unguiculata*)

Journal:	<i>Environmental Science & Technology</i>
Manuscript ID:	es-2013-03466p.R2
Manuscript Type:	Article
Date Submitted by the Author:	26-Oct-2013
Complete List of Authors:	Wang, Peng; The University of Queensland, School of Agriculture and Food Sciences Menzies, Neal; The University of Queensland, Lombi, Enzo; University of South Australia, Centre for Environmental Risk Assessment and Remediation McKenna, Brigid; The University of Queensland, Johannessen, Bernt; Australian Synchrotron, Glover, Chris; Australian Synchrotron, Kappen, Peter; Australian Synchrotron, Kopittke, Peter; The University of Queensland, ; The University of Queensland,

SCHOLARONE™
Manuscripts

Fate of ZnO nanoparticles in soils and cowpea (*Vigna unguiculata*)

Peng Wang,^{†,} Neal W. Menzies,[†] Enzo Lombi,[‡] Brigid A. McKenna,[†] Bernt Johannessen,[§] Chris J. Glover,[§] Peter Kappen,[§] and Peter M. Kopittke[†]*

[†]School of Agriculture and Food Sciences, The University of Queensland, St. Lucia, Queensland, 4072, Australia

[‡]Centre for Environmental Risk Assessment and Remediation, University of South Australia, Mawson Lakes, South Australia, 5095, Australia

[§]Australian Synchrotron, Clayton, Victoria, 3168, Australia

*To whom correspondence should be addressed. Phone: +61 7 3365 4816, Fax: +61 7 3365 1177, Email:

p.wang3@uq.edu.au

1 Abstract

2 The increasing use of zinc oxide nanoparticles (ZnO-NPs) in various commercial products is prompting
3 detailed investigation regarding the fate of these materials in the environment. There is, however, a lack
4 of information comparing the transformation of ZnO-NPs with soluble Zn²⁺ in both soils and plants.
5 Synchrotron-based techniques were used to examine the uptake and transformation of Zn in various
6 tissues of cowpea (*Vigna unguiculata* (L.) Walp.) exposed to ZnO-NPs or ZnCl₂ following growth in
7 either solution or soil culture. In solution culture, soluble Zn (ZnCl₂) was more toxic than the ZnO-NPs,
8 although there was substantial accumulation of ZnO-NPs on the root surface. When grown in soil,
9 however, there was no significant difference in plant growth and accumulation or speciation of Zn
10 between soluble Zn and ZnO-NP treatments, indicating that the added ZnO-NPs underwent rapid
11 dissolution following their entry into the soil. This was confirmed by an incubation experiment with two
12 soils, in which ZnO-NPs could not be detected after incubation for 1 h. The speciation of Zn was similar
13 in shoot tissues for both soluble Zn and ZnO-NPs treatments and no upward translocation of ZnO-NPs
14 from roots to shoots was observed in either solution or soil culture. Under the current experimental
15 conditions, the similarity in uptake and toxicity of Zn from ZnO-NPs and soluble Zn in soils indicates that
16 the ZnO-NPs used in this study did not constitute nano-specific risks.

17

18 **Keywords:** ZnO nanoparticles, uptake, toxicity, transformation, soil, plant, zinc

19 INTRODUCTION

20 Engineered nanoparticles (ENPs) are being developed and incorporated into a variety of industrial,
21 commercial, and medicinal products. Zinc oxide nanoparticles (ZnO-NPs) are among the most commonly
22 used ENPs in personal care products (e.g. sunscreens, cosmetics), textiles, paintings, industrial coatings,
23 dye-sensitized solar cells, antibacterial agents, and optic and electronic materials.¹ In addition, ZnO-NPs
24 have been proposed as an effective Zn fertilizer to alleviate Zn deficiency in soils.² While some of these
25 commercial applications, and their relative exposure pathways (e.g. through the wastewater treatment
26 process), are unlikely to lead to the direct release of ZnO-NPs to the environment, others (e.g. fertilisers)
27 could lead to their direct release to the soil. As a novel and emerging class of products, the ecological risk
28 of ZnO-NPs is an important topic that is receiving increased scrutiny from both the scientific and
29 regulatory viewpoints.

30

31 Plants are an important component of the ecological system and serve as a potential pathway for the
32 transportation and accumulation of ENPs into the food chain.³⁻⁵ There is evidence that particles up to 20
33 nm are taken up by plant cells through plasmodesmata and endocytosis.⁶ Indeed, some studies have
34 demonstrated the uptake of ENPs by plants grown in solution culture. For example, Lin and Xing⁷ used
35 transmission electron microscopy (TEM) to show that ZnO-NPs passed through the epidermis and cortex
36 of roots of *Lolium perenne* L. (ryegrass), but did not examine if they are present within the shoots. Zhu et
37 al.³ used magnetization to show the uptake and subsequent transport of magnetite Fe₃O₄-NPs by
38 *Cucurbita maxima* (pumpkin) grown in solution culture. However, no Fe₃O₄-NPs (i.e. magnetic signals)
39 were detected in shoots of soil-cultured plants. This is similar to other soil- or sand-based studies, which
40 were unable to detect plant uptake of NPs. For example, no ZnO-NPs were detected in either roots⁸ or
41 shoots⁹ of wheat (*Triticum aestivum* L.) or in stems and pods of soybean (*Glycine max* (L.) Merr.)¹⁰, and
42 no CeO₂ NPs were detected in leaves of maize (*Zea mays* L.).¹¹ These findings suggest that the growth
43 matrix affects the uptake of NPs, but, to our knowledge, there are no data quantifying the differences in
44 the uptake and transformation (i.e. the chemical form) of ZnO-NPs in various tissues of plants grown in
45 different growth matrices.

46

47 The absence of ZnO-NPs in shoots may be explained by their attachment to the soil particles or the rapid
48 dissolution and transformation of ZnO-NPs upon entering the soil. Indeed, it has been suggested that
49 ZnO-NPs undergo quick dissolution/transformation upon their release into the environment.¹²⁻¹⁵ Although
50 most ZnO-NPs released from consumer products are likely converted to other species before entering the
51 soil as applied biosolids,¹³ the application of ZnO-NPs as a Zn fertilizer (including as a foliar fertilizer)
52 has also been proposed.² Indeed, there is growing interest in the use of ZnO-NPs as fertilizers as Zn
53 deficiency is by far the most widespread micronutrient deficiency limiting crop production in the world.¹⁶
54 In the case of soils, however, little is known about the fate of ZnO-NPs over time.

55

56 The aims of this study were (i) to compare the uptake and toxicity (and subsequent transformation) of
57 ZnO-NPs and ZnCl₂ to inform the associated environmental risks, and (ii) to determine if there are any
58 differences between the uptake of the Zn in soil or solution culture. In this study, we examined the
59 speciation of Zn within various tissues of plants exposed to ZnO-NPs or ZnCl₂ in solution or soil culture
60 and assessed the fate of ZnO-NPs over time in two soils (differing in chemical and physical properties).

61

62 MATERIALS AND METHODS

63 **Zinc Oxide Nanoparticles.** The ZnO-NP dispersion, synthesized by the hydrolysis of a zinc salt in a
64 polyol medium heated to 160 °C, was purchased from Sigma Aldrich (catalog No. 721077). This product
65 has a reported particle size < 100 nm measured by dynamic light scattering (DLS) and an average particle
66 size < 35 nm measured using an aerodynamic particle sizer (APS) spectrometer. Our analyses of the
67 suspensions used for the experiments by DLS using a Zetasizer Nano (Malvern Instruments,
68 Worcestershire, UK) gave an average number-weighted particle size of 67 ± 2 nm and zeta potential of
69 $+46.1 \pm 1.5$ mV. Images analysed by field emission scanning electron microscopy (SEM, JEOL JSM
70 6400 F) indicated a crystallite size range of 20–30 nm.

71

72 **Plant Growth Conditions.** Both solution and soil culture experiments were conducted simultaneously in
73 a semi-controlled glasshouse in full sunlight at The University of Queensland, St Lucia, Australia. The
74 temperature was maintained at ca. 28°C during the day and 20°C during the night. Relative humidity
75 typically ranged between 25 and 50% during the day and 60 to 80% during the night.

76

77 *Solution Culture.* Seeds of cowpea (*Vigna unguiculata* (L.) Walp. cv. Red Caloona) were germinated in
78 trays covered with paper towel moistened with tap water. After 2 d, seedlings were transferred to
79 containers with 11 L of nutrient solution (μM): 800 NO_3^- -N, 120 NH_4^+ -N, 650 Ca, 100 Mg, 300 K, 550
80 SO_4^{2-} -S, 140 Cl, 10 P, 10 Fe (supplied as Fe(III)CDTA), 3.0 B, 1.0 Mn, 0.05 Cu, 0.01 Zn, and 0.02 Mo.
81 Solution pH was not adjusted but averaged pH 6.1. After a further 3 d, four seedlings were transferred to
82 four replications of 11 L solutions (as above) containing no added Zn (control) or with Zn added as either
83 ZnO-NPs or ZnCl_2 to achieve a final concentration of 25 mg Zn L^{-1} (38.2 μM). This Zn concentration has
84 been shown to reduce root growth by approximately 70%¹⁷ and is within the range found in soil
85 solutions.¹⁸ Solutions were continuously aerated and renewed every 4 d, with plants harvested after 4
86 weeks. At harvest, the roots were washed with flowing deionized water for ca. 1 min and blotted dry with
87 filter paper, before the roots, stems, and leaves were separated. Subsamples of each tissue were immersed
88 in liquid nitrogen and immediately stored in a dry shipper cooled with liquid nitrogen for later analysis
89 using X-ray absorption spectroscopy (XAS). The remaining tissues were oven-dried for analysis using
90 inductively coupled plasma mass spectrometry (ICP-MS) (details provided below).

91

92 *Soil Culture.* An Oxisol (US Soil Taxonomy) with pH 6.7 and a sandy clay texture, collected from a site
93 near Toowoomba, Queensland (Table S1), was air-dried and sieved to < 2 mm. The soil was amended
94 with either ZnO-NPs or ZnCl_2 with a target concentration of 500 mg Zn kg^{-1} soil as used by Priester et
95 al.¹⁹ This concentration is far in excess of that expected under a fertilisation scenario and could only be
96 conceived to result from an unintentional spill of concentrated ZnO-NP solutions. However, this is the
97 highest concentration used by Priester et al.¹⁹ reporting a negative impact of ENPs on soil fertility and
98 soybean growth. As pointed out by Lombi et al.²⁰, the above-mentioned article did not include a soluble

99 Zn treatment and it was therefore not possible to draw any definitive conclusion regarding any nano-
100 specific effects with regard to toxicity. In this article, we provide such comparison which is essential in
101 the context of the debate regarding the environmental consequence of nanotechnologies. To ensure even
102 distribution of Zn in the soil, the ZnO-NP suspensions or ZnCl₂ solutions (20 mg Zn mL⁻¹) were diluted
103 with deionized water to a volume of 50 mL and sprayed over 2 kg dry soil which was then mixed
104 thoroughly by hand. A control (no added Zn) was also included by spraying with the same volume of
105 deionized water. Each treatment was replicated three times with 2.0 kg soil in each 4 L plastic pot. Soils
106 were watered to 60% of water holding capacity and equilibrated for 1 d prior to planting. Six 3-d old
107 seedlings were transferred to each pot and three seedlings harvested after 4 weeks. The shoots were rinsed
108 with deionized water and separated into stems and leaves. The root system was removed by carefully
109 breaking apart the soil and then rinsing with deionized water for ca. 1 min, blotted dry, and separated into
110 roots and nodules. Samples of each tissue were immersed in liquid nitrogen and stored in a dry shipper for
111 later analysis using XAS. The remaining samples were oven-dried for analysis using ICP-MS. The
112 remaining three plants in each pot were harvested at maturity (ca. 80 d after planting) and samples of
113 seeds ground to fine powder for later analysis using XAS and ICP-MS.

114

115 **Soil Incubation Experiment.** The fate of ZnO-NPs following addition to soil was investigated in the
116 Oxisol (described above) and in an Ultisol (US Soil Taxonomy) collected from the Central Highlands of
117 Queensland. This soil is an acidic (pH 5.0) sandy loam soil (Table S1). Two replicates (100 g) of both
118 soils were amended with ZnO-NPs or ZnCl₂ to a target concentration of 500 mg kg⁻¹ soil as described
119 above, placed in 300 mL beakers, and deionized water added to 60% of soil water holding capacity. Each
120 beaker was covered and sealed with plastic film with small holes to maintain relatively constant moisture;
121 deionized water was added every 4 d if necessary. Soils were incubated in the dark at 25 ± 2°C, and
122 samples collected after 1 h, 1 d, 5 d, and 15 d, immediately frozen (ca. -20°C), and later freeze-dried for
123 analysis using XAS.

124

125 **Bulk XAS.** Zinc K_{α} -edge X-ray absorption near edge structure (XANES) and extended X-ray absorption
126 fine structure (EXAFS) spectra were collected at the XAS Beamline at the Australian Synchrotron,
127 Melbourne as described by Kopittke et al.²¹ The energy of each spectrum was calibrated by simultaneous
128 measurement in transmission mode of a metallic Zn foil reference (K_{α} -edge at 9,659 eV). The spectra
129 were collected in fluorescence mode with a 100-element solid-state Ge detector. To prepare samples, ca.
130 1-2 g frozen plant tissues were homogenized in an agate mortar and pestle continuously cooled with
131 liquid nitrogen.¹⁷ Soil and seed samples were ground using a mortar and pestle and sieved to < 250 μm
132 using a stainless steel sieve. A total of 29 Zn standards was also examined, including six aqueous
133 compounds²¹ and 23 finely ground powder spectra¹³. The aqueous standards were used for fitting Zn
134 ligands in plant tissues and the solid standards for Zn ligands in soils. Due to the low concentration of Zn
135 in some fresh plant samples, only XANES spectra were collected for plant samples, while both XANES
136 and EXAFS spectra were collected for soil samples. The spectra (average of three scans) were energy
137 normalized using Athena software.²² Principal component analysis (PCA) of the normalized sample
138 spectra was used to estimate the likely number of species contained in the samples, while target
139 transformation (TT) was used to identify relevant standards for linear combination fitting (LCF) of the
140 sample spectra.²³ PCA and TT were undertaken using SixPack.²⁴ For both XANES (-20 to +30 E, eV) and
141 EXAFS (2.5 to 9 k, \AA^{-1}), LCF was performed using Athena.

142

143 **X-ray Fluorescence Microscopy (μ -XRF).** Elemental μ -XRF maps were collected at the XFM Beamline
144 at the Australian Synchrotron²⁵ using roots exposed to 25 mg Zn L^{-1} as ZnO-NPs or ZnCl_2 for 1 d. In
145 addition, mature seeds of plants grown in the Oxisol amended with ZnO-NPs or ZnCl_2 were
146 longitudinally sliced (ca. 200 μm) for μ -XRF analysis. The XRF spectra were analyzed using GeoPIXE²⁶
147 and the images were generated using the Dynamic Analysis method.²⁷

148

149 **Digestion and Analysis of Total Zn.** Dry plant tissues were placed into 50 mL conical flasks and
150 digested using 10 mL 5:1 HNO_3 : HClO_4 . Following digestion, the samples were diluted to 10 mL using
151 deionized water before analysis by ICP-MS. Soil samples were digested with aqua regia (1:3 HCl : HNO_3)

152 and analyzed for total Zn by ICP-MS. Quality control measures included the use of procedural blanks and
153 repeat analysis of a certified reference.

154

155 **Statistical Analysis.** Treatment-differences were tested for significance ($p < 0.05$) using a one-way
156 analysis of variance (ANOVA) performed with IBM SPSS Statistics 20.

157

158 **RESULTS**

159 **ZnO-NPs and Soluble Zn Effects on Plants.** In solution culture, the addition of Zn reduced plant growth
160 compared to that in the control (basal nutrient solution), with toxicity more severe in ZnCl₂ solutions than
161 with those containing ZnO-NPs (Table S2). In contrast, there were no significant effects ($p > 0.05$) on
162 plant growth between the control and the ZnO-NP and ZnCl₂ treatments in soil culture.

163

164 After 4 weeks in solution culture, Zn concentration in roots exposed to ZnO-NPs (44,700 $\mu\text{g g}^{-1}$ dry mass,
165 DM) was 4.6-times higher than those exposed to ZnCl₂ (9,650 $\mu\text{g g}^{-1}$ DM). Concentrations in stems (487
166 and 584 $\mu\text{g g}^{-1}$ DM) and leaves (119 and 139 $\mu\text{g g}^{-1}$ DM) were similar between the ZnO-NP and ZnCl₂
167 treatments (Table S3). As a consequence, the Zn transfer coefficient (i.e. the ratio of Zn in the leaf
168 relative to the root) was 4.7-times lower in the ZnO-NP treatment (0.003) compared to that in the ZnCl₂
169 treatment (0.014). This similarity indicated that the increased accumulation of Zn in roots exposed to
170 ZnO-NPs in solution culture is likely due to either an increased adhesion or limited transport of ZnO-NPs
171 to the shoot. In the case of soil culture, there were no significant differences ($p > 0.05$) in Zn
172 concentrations of roots (1,003 and 1,180 $\mu\text{g g}^{-1}$ DM), stems (108 and 118 $\mu\text{g g}^{-1}$ DM), leaves (155 and
173 181 $\mu\text{g g}^{-1}$ DM), or seeds (43.3 and 55.7 $\mu\text{g g}^{-1}$ DM) between the ZnO-NP and ZnCl₂ treatments (Table
174 S3). Transfer coefficients in soil culture (0.155 and 0.154) were substantially higher than those in solution
175 culture.

176

177 **Zinc Speciation and Distribution in Plant Tissues.** The Zn XANES spectrum for ZnO-NPs (Figure 1)
178 is readily identified due to its unique features, particularly the shoulder at 9,780 eV, and is similar to

179 previously-reported spectra for this material.^{13, 14} The Zn XANES spectra for all other standards, while
180 different from each other, were substantially different from that of ZnO-NPs.
181

182 Overall, it was apparent that the XANES spectra of roots exposed to ZnO-NPs in solution culture were
183 markedly different from that obtained for the ZnCl₂-exposed roots, with the spectrum for ZnO-NP-
184 exposed roots resembling that of the ZnO-NPs themselves (Figure 1A). It would appear that ZnO-NPs
185 were the primary form of Zn in these samples – this being supported by the distribution of Zn using μ -
186 XRF. Zinc was largely located on the root surface, most likely due to the adhesion and aggregation of
187 ZnO-NPs (Figure 2A). Indeed, LCF revealed that ca. 65% of the Zn in these ZnO-NP-exposed roots was
188 present as ZnO-NPs, with 32% associated with histidine (Table 1). In contrast, roots exposed to ZnCl₂ in
189 solution culture accumulated Zn in the root apex (i.e. meristematic zone) (Figure 2A). This Zn was found
190 to be associated with histidine (49%) and polygalacturonic acid (Zn-PGA, 32%), and Zn-phosphate (19%).
191

192 Interestingly, and in contrast to the solution culture results, the XANES spectra of roots grown in soil
193 were similar regardless of whether the roots were exposed ZnO-NPs or ZnCl₂ (Figure 1B). Using LCF,
194 the Zn in roots from these ZnO-NP and ZnCl₂ treatments was found to be associated with citrate (average
195 51%), histidine (28%), and phytate (20%) (Table 1). Given the similar concentration of Zn in roots
196 exposed to ZnO-NPs and ZnCl₂ (Table S3), it is possible that the ZnO-NPs underwent dissolution in the
197 soil.
198

199 The XANES spectra obtained for the stems and leaves from the ZnO-NP and ZnCl₂ treatments in both
200 solution and soil culture were visually similar to the spectrum of Zn citrate (Figure 1). This observation
201 was confirmed by LCF, with the Zn in these tissues mainly associated with citrate (50%), histidine (26%),
202 and phytate (24%) (Table 1). In the root nodules, Zn was associated with citrate (37%), phytate (38%),
203 and cysteine (27%) (Table 1).
204

205 The XANES spectra for seeds of plants grown in the ZnO-NP and ZnCl₂ treatments in soil showed a
206 characteristic broader double-peaked feature, which resembled the Zn phytate spectrum in some regards
207 (Figure 1B). However, the best fits using LCF included association with three components, histidine
208 (50%), cysteine (30%) and phosphate (20%) (Table 1). Even if Zn phytate was included as one of the
209 standards in the LCF, only 16-33% was calculated to be presented as Zn phytate, with the remainder of
210 Zn present associated with cysteine (40-47%) and histidine (26-37%) (the R-factors increasing by 50 to
211 100% compared to the best fits). Therefore, ca. 70 to 80% of the Zn in the seeds was associated with
212 amino acids (i.e. histidine and cysteine), with 20 to 30% bound to phosphate such as Zn₃(PO₄)₂ or as Zn
213 phytate. The spatial distribution of Zn within the seeds determined using μ-XRF was found to be similar
214 in the ZnO-NP and ZnCl₂ treatments. A high concentration of Zn was evident in the outer layer of
215 cotyledon and the hypocotyl, with low Zn concentration in the seed coat (testa) and the inner cotyledon
216 (Figure 2B).

217

218 **Zinc Speciation in Soils.**

219 Across the incubation periods examined, both XANES and EXAFS spectra were similar regardless of
220 whether the soils were amended with ZnCl₂ or ZnO-NPs (Figure 3 and Table 2), indicating a rapid
221 dissolution of the ZnO-NPs and that incubation for up to 15 d did not substantially change the speciation
222 of Zn in either soil. In the Oxisol with ZnCl₂, LCF using the XANES spectra indicated that the Zn was
223 present as Zn sorbed ferrihydrite (54%), ZnAl-layered double hydroxide (ZnAl-LDH) (22%), and ZnSO₄
224 (23%). In the case of the Ultisol, 35% of the Zn was calculated to be in a form resembling hopeite
225 (Zn₃(PO₄)₂), with Zn also present as ZnAl-LDH (14%), Zn-humic acid (21%), and ZnSO₄ (30%) (Figure
226 3 and Table 2). These results regarding the presence of ZnAl-LDH and ZnSO₄ were reinforced by
227 analysis of the EXAFS spectra (Table 2). Indeed, for both soils, LCF of the EXAFS spectra indicated that
228 the Zn was present as 43% of hemimorphite (Zn₄Si₂O₇(OH)₂·H₂O), 29% as ZnAl-LDH, and 28% as
229 ZnSO₄ (Table 2). The slight discrepancy between XANES and EXAFS LCF results has been reported
230 previously^{28,29} and could be related to the lower sensitivity of EXAFS to metals bound to matrices
231 composed of light elements or organic matter.²⁸

232

233 Even when ZnO-NPs were added into the soil, almost all of the Zn was present in the same forms as when
234 ZnCl₂ was added (Figure 3 and Table 2). The LCF of the XANES spectra for both soils revealed that no
235 Zn could be detected in the form of ZnO-NPs after 1 h incubation. These results suggest that the large
236 majority of the added ZnO-NPs underwent rapid dissolution following their entry into the soils. It should
237 be noted, however, that changes in Zn speciation may have occurred during the time between the samples
238 being transferred to -20 °C and their freezing.

239

240 DISCUSSION

241 In solution culture, soluble Zn (ZnCl₂) was more toxic than ZnO-NPs to the growth of cowpea (Table S2)
242 despite the apparent accumulation of ZnO-NPs on the root surface (Figure 2 and Table S3). Interestingly,
243 however, when grown in soil, there was no difference in plant growth between the ZnCl₂ and ZnO-NP
244 treatments (Table S2). This difference between solution and soil culture highlights the importance of the
245 growth matrix in plant culture experiments. Importantly, it was noted that there was also no significant
246 difference in Zn concentration in shoots between the ZnCl₂ and ZnO-NPs treatments (Table S3) and we
247 did not detect the upward translocation of ZnO-NPs from roots to shoots of plants grown in either
248 solution or soil culture (Table 1 and Figure 1). Under the current experimental conditions, the ZnO-NPs
249 added to the soil were rapidly converted to the same forms as when ZnCl₂ was added (Figure 3 and Table
250 2). This indicates that even at the high rate of ZnO-NPs added in the current study, no nano-specific
251 effects (toxicity, uptake, speciation, and distribution) could be observed when plants were grown in soils.
252 Thus, whilst Priester et al.¹⁹ reported that the use of ZnO-NPs may result in “agriculturally associated
253 human and environmental risks”, our data suggest that these risks for ZnO-NPs, under the current
254 experimental conditions, would not differ from those of soluble Zn. It is noteworthy that Priester et
255 al.¹⁹ did not include a soluble Zn control in their study.

256

257 In solution culture, accumulation of Zn in roots exposed to ZnO-NPs was 4.6-times higher than that in the
258 ZnCl₂ treatment, but toxicity was more severe in solutions with ZnCl₂ (Tables S2 and S3). The majority

259 of the Zn in roots exposed to ZnO-NPs was on the root surface due to their adhesion and aggregation
260 (Figure 2A). Indeed, the XAS analyses indicated that ca. 65% of Zn in these roots was present as ZnO-
261 NPs (Table 1 and Figure 1). In addition, the speciation of Zn was similar in the shoots for both ZnCl₂ and
262 ZnO-NP treatments and no ZnO-NPs were detected in shoot tissues despite the substantial accumulation
263 of ZnO-NPs on the root surface (Table 1 and Figure 1). These observations indicate that the Zn uptake
264 and toxicity was due to particle dissolution in the bulk nutrient solution and particle adhesion onto the
265 root surface, rather than the uptake of nanoparticles. These findings are in accordance with previous
266 reports^{12, 30-32} which concluded that the toxicity of ZnO-NPs is due solely to solubilized Zn²⁺.

267

268 In soil culture, there was no significant difference in plant growth or uptake of Zn between the two Zn
269 treatments (Table S2 and S3). There was rapid equilibration through adsorption and precipitation
270 reactions upon addition of soluble ZnCl₂ or ZnO-NPs to soil. This could be seen by the presence of ZnAl-
271 LDH, hopeite, and hemimorphite (Table 2), the formation of which substantially reduced the toxicity of
272 Zn to the plants. In addition, the phytotoxicity of Zn in soils depends on a range of soil properties
273 (including pH and cation exchange capacity [CEC]). Indeed, Smolders et al.³³ reported that the EC10
274 (10% effective concentration) values for *Triticum aestivum* grown in a range of soils varied from 9 to
275 1,231 mg kg⁻¹ (cf. 500 mg kg⁻¹ used in pot experiment with a pH-neutral soil). The application of ZnO-
276 NPs to the Oxisol (pH-neutral) and Ultisol (acidic) had similar effects to that of ZnCl₂ with no ZnO-NPs
277 detected after incubating for 1 h (Table 2 and Figure 3). This finding suggests a rapid dissolution of ZnO-
278 NPs in these soils, most likely driven by sorption of solubilized Zn²⁺ found in previous studies.^{13, 14, 34-36}
279 For example, Lombi et al.¹³ found that ZnO-NPs in sewage sludge were converted to ZnS within 1 d.
280 Similarly, Scheckel et al.¹⁴ found that the addition of a clay mineral (kaolinite) resulted in the dissolution
281 of ZnO-NPs within 1 d due to their sorption to the negative charge of the clay (78% of the ZnO-NPs
282 sorbed within 1 h). Given that kaolinite has a similar (or lower) CEC (ca. 1-5 cmol_c/kg) relative to the
283 soils used in the present study (2.3 or 13 cmol_c/kg, see Table S1), the observation that the ZnO-NPs
284 underwent rapid dissolution upon their addition to the soils is in accordance with previous findings.
285 However, it seems that the speed of dissolution of ZnO-NPs depends upon soil properties (particularly pH)

286 and the method used to add ZnO-NPs to the soil. For example, in contrast to the present study where
287 ZnO-NPs could not be detected after 1 h in acidic soils, Collins et al.³⁶ found that dissolution of the ZnO-
288 NPs required 30 d after sprinkling nanoparticles on the surface of an alkaline soil (pH 7.5). Similarly,
289 using flow field-flow fractionation, Gimbert et al.³⁷ was still able to detect ZnO-NPs in suspensions of an
290 alkaline soil (pH 9.0) spiked with 12,000 mg Zn kg⁻¹ after 14 d incubation.

291

292 In the present study, no ZnO-NPs were detected in any shoot tissues regardless of growth matrix (Table 1
293 and Figure 1), indicating no transfer of ZnO-NPs from roots to shoots. This finding is in keeping with
294 recent studies in which no ZnO-NPs could be detected in shoots of soil-grown soybean using XAS; rather,
295 Zn was associated with citrate in the stem and seed pod¹⁰. Additionally, Zn phosphate was present in the
296 shoots of wheat grown with added ZnO-NPs in sand culture.⁹

297

298 In roots exposed to ZnCl₂ in solution culture, the majority of the Zn was observed in the meristemic
299 region (Figure 2A) and LCF analysis indicated that the Zn was primarily associated with histidine, with
300 slightly smaller contributions from polygalacturonic acid (the main component of pectin in the cell wall)
301 and precipitated as Zn-phosphate (Table 1). This suggests that histidine and the cell wall play important
302 roles in Zn homeostasis and detoxification in roots. Similarly, Salt et al.³⁸ reported that the majority of the
303 intracellular Zn in roots of *Thlaspi caerulescens*, a Zn hyperaccumulator, grown in solution culture was
304 coordinated with histidine, with the remainder complexed to the cell wall. In the present study, however,
305 no Zn was found to be present as Zn-phosphate within roots when grown in soil culture, but rather was
306 associated with citrate, histidine, and phytate (Table 1). Zinc-phosphate precipitates have been observed
307 at the surface of roots grown in solution culture^{39,40}, being most likely related to the low transfer
308 coefficients of Zn from root to shoot (Table S3). This is consistent with the observations by Sarret et al.⁴¹
309 with Zn in *Arabidopsis halleri* grown in solution culture.

310

311 Organic acids including citrate, malate, and oxalate are primarily located in the vacuoles⁴² and are often
312 found to chelate Zn in leaves⁴³ and as found by Salt et al.³⁸ with citrate in shoots of *T. caerulescens*. In

313 the present study, we found that the chemical forms of Zn were similar in all stem and leaf tissues
314 regardless of Zn-treatments, with Zn mainly bound to citrate, histidine, and phytate (Table 1). It is not
315 possible to exclude the presence of other compounds with carboxyl groups (e.g. malate), but our results
316 support the role of carboxyl groups as important ligands involved in the transport and storage of Zn in
317 shoots.^{38, 43}

318

319 Surprisingly, there is comparatively little information regarding the speciation of Zn in seeds. The LCF
320 results revealed that ca. 80% of the Zn was coordinated with amino acids such as histidine and cysteine,
321 with a smaller proportion precipitated with phosphate (Table 1). Phytic acid has been found to be the
322 main storage form of P in cereals⁴⁴, and that phytate has a high affinity for Zn, Fe, and other trace
323 elements.⁴⁵ The co-localization of phytate with these elements⁴⁶ seems to support the hypothesis that
324 phytate plays an important role in the storage of Zn in the seeds or grains. However, LCF results in the
325 present study (Table 1) showed that Zn was predominantly associated with amino acids (histidine and
326 cysteine). Indeed, the importance of amino acids (c.f. phytate) for Zn storage has been reported previously
327 in barley (*Hordeum vulgare* L.) grain. For example, Persson et al.⁴⁷ incubated barley grain with phytase
328 which degrades phytate, a treatment that doubled the extraction efficiency of P but have no effect on that
329 of Zn. Rather, Zn was found to be bound mainly to peptides as measured using SEC/IP-ICP-MS.
330 Similarly, in a study with low-phytate barley grain mutants, Hatzack et al.⁴⁸ found that impaired phytate
331 accumulation did not influence Zn storage capacity in the grains.

332

333 Limitations of the XAS techniques employed in this study include uncertainty in species of ca. 5% of the
334 total amount of the target element^{49, 50} which may result in the XAS analysis being insufficiently
335 sensitive to identify small amounts of ZnO-NPs in plants and in soils.

336

337 In summary, we have not detected the translocation of ZnO-NPs from roots to shoots of plants grown in
338 either solution or soil culture, although there was a substantial quantity of ZnO-NPs on the surface of
339 roots exposed to ZnO-NP in solution culture. Even though large quantities of pristine NPs were applied

340 directly to the soil with which they were mixed thoroughly, the ZnO-NPs appeared to be completely
341 dissociated after 1 h incubation and transformed in similar manner to the ZnCl₂ treatment. Indeed, there
342 was no significant difference between the ZnO-NP and ZnCl₂ treatments in plant growth, Zn
343 accumulation, or Zn speciation in plant tissues. We conclude, therefore, that under the current
344 experimental conditions, there were no nano-specific effects on plants grown in soil, and that this finding
345 needs to be considered in environmental risk assessment and management strategies.

346

347 **ASSOCIATED CONTENT**

348 **Supporting Information**

349 Additional information is available regarding the characteristics of soils used in this study, cowpea
350 biomass, Zn concentration in various plant tissues, results of the PCA analysis, target transformation
351 SPOIL values of reference spectra, and the Fourier Transform of EXAFS spectra for all soil samples. This
352 material is available free of charge via the Internet at <http://pubs.acs.org>.

353

354 **AUTHOR INFORMATION**

355 **Corresponding Author**

356 *Email: p.wang3@uq.edu.au; tel: +61 7 3365 4816; fax: +61 7 3365 1177.

357

358 **Notes**

359 The authors declare no competing financial interest.

360

361 **ACKNOWLEDGEMENTS**

362 This research was mainly undertaken at the XAS (AS123/XFM/5349) and XFM (AS131/XAS/5723)
363 Beamlines at the Australian Synchrotron, Victoria, Australia. Support was provided to Dr Wang as a
364 recipient of an Australian Research Council (ARC) DECRA (DE130100943) and to Dr Kopittke and Prof
365 Lombi as recipients of ARC Future Fellowships (FT120100277 and FT100100337, respectively). This
366 research was also supported under the ARC Linkage Projects funding scheme (LP130100741).

367

368 **REFERENCES**

- 369 1. Ju-Nam, Y.; Lead, J. R., Manufactured nanoparticles: An overview of their chemistry, interactions
370 and potential environmental implications. *Sci. Total Environ.* **2008**, *400* (1-3), 396-414.
- 371 2. Milani, N.; McLaughlin, M. J.; Stacey, S. P.; Kirby, J. K.; Hettiarachchi, G. M.; Beak, D. G.;
372 Cornelis, G., Dissolution kinetics of macronutrient fertilizers coated with manufactured zinc oxide
373 nanoparticles. *J. Agr. Food Chem.* **2012**, *60* (16), 3991-3998.
- 374 3. Zhu, H.; Han, J.; Xiao, J. Q.; Jin, Y., Uptake, translocation, and accumulation of manufactured iron
375 oxide nanoparticles by pumpkin plants. *J. Environ. Monitor.* **2008**, *10* (6), 713-717.
- 376 4. Unrine, J. M.; Shoults-Wilson, W. A.; Zhurbich, O.; Bertsch, P. M.; Tsyusko, O., Trophic transfer of
377 Au nanoparticles from soil along a simulated terrestrial food chain. *Environ. Sci. Technol.* **2012**, *46*
378 (7), 9357-9360.
- 379 5. Ma, X.; Geiser-Lee, J.; Deng, Y.; Kolmakov, A., Interactions between engineered nanoparticles
380 (ENPs) and plants: Phytotoxicity, uptake and accumulation. *Sci. Total Environ.* **2010**, *408* (16), 3053-
381 3061.
- 382 6. Dietz, K.-J.; Herth, S., Plant nanotoxicology. *Trends Plant Sci.* **2011**, *16* (11), 582-589.
- 383 7. Lin, D. H.; Xing, B. S., Root uptake and phytotoxicity of ZnO nanoparticles. *Environ. Sci. Technol.*
384 **2008**, *42* (15), 5580-5585.
- 385 8. Du, W.; Sun, Y.; Ji, R.; Zhu, J.; Wu, J.; Guo, H., TiO₂ and ZnO nanoparticles negatively affect wheat
386 growth and soil enzyme activities in agricultural soil. *J. Environ. Monitor.* **2011**, *13* (4), 822-828.
- 387 9. Dimkpa, C. O.; Latta, D. E.; McLean, J. E.; Britt, D. W.; Boyanov, M. I.; Anderson, A. J., Fate of
388 CuO and ZnO nano- and microparticles in the plant environment. *Environ. Sci. Technol.* **2013**, *47* (9),
389 4734-4742.
- 390 10. Hernandez-Viezcas, J. A.; Castillo-Michel, H.; Andrews, J. C.; Cotte, M.; Rico, C.; Peralta-Videa, J.
391 R.; Ge, Y.; Priester, J. H.; Holden, P. A.; Gardea-Torresdey, J. L., In situ synchrotron X-ray
392 fluorescence mapping and speciation of CeO₂ and ZnO nanoparticles in soil cultivated soybean
393 (*Glycine max*). *ACS Nano* **2013**, *7* (2), 1415-1423.
- 394 11. Birbaum, K.; Brogioli, R.; Schellenberg, M.; Martinoia, E.; Stark, W. J.; Günther, D.; Limbach, L. K.,
395 No evidence for cerium dioxide nanoparticle translocation in maize plants. *Environ. Sci. Technol.*
396 **2010**, *44* (22), 8718-8723.
- 397 12. Brunner, T. J.; Wick, P.; Manser, P.; Spohn, P.; Grass, R. N.; Limbach, L. K.; Bruinink, A.; Stark, W.
398 J., In vitro cytotoxicity of oxide nanoparticles: □ Comparison to asbestos, silica, and the effect of
399 particle solubility. *Environ. Sci. Technol.* **2006**, *40* (14), 4374-4381.

- 400 13. Lombi, E.; Donner, E.; Tavakkoli, E.; Turney, T.; Naidu, R.; Miller, B. W.; Scheckel, K. G., Fate of
401 zinc oxide nanoparticles during anaerobic digestion of wastewater and post-treatment processing of
402 sewage sludge. *Environ. Sci. Technol.* **2012**, *46* (16), 9089-9096.
- 403 14. Scheckel, K. G.; Luxton, T. P.; El Badawy, A. M.; Impellitteri, C. A.; Tolaymat, T. M., Synchrotron
404 speciation of silver and zinc oxide nanoparticles aged in a kaolin suspension. *Environ. Sci. Technol.*
405 **2010**, *44* (4), 1307-1312.
- 406 15. Reed, R. B.; Ladner, D. A.; Higgins, C. P.; Westerhoff, P.; Ranville, J. F., Solubility of nano-zinc
407 oxide in environmentally and biologically important matrices. *Environ. Toxicol. Chem.* **2012**, *31* (1),
408 93-99.
- 409 16. Alloway, B.; Graham, R.; Stacey, S., Micronutrient Deficiencies in Australian Field Crops. In
410 *Micronutrient Deficiencies in Global Crop Production*, Alloway, B., Ed. Springer Netherlands: 2008;
411 pp 63-92.
- 412 17. Kopittke, P. M.; Blamey, F. P. C.; McKenna, B. A.; Wang, P.; Menzies, N. W., Toxicity of metals to
413 roots of cowpea in relation to their binding strength. *Environ. Toxicol. Chem.* **2011**, *30* (8), 1827-
414 1833.
- 415 18. Schwab, A. P., The soil solution. In *Handbook of Soil Science*, Sumner, M. E., Ed. CRC Press: New
416 York, 2000; pp B85-B88.
- 417 19. Priester, J. H.; Ge, Y.; Mielke, R. E.; Horst, A. M.; Moritz, S. C.; Espinosa, K.; Gelb, J.; Walker, S.
418 L.; Nisbet, R. M.; An, Y.-J.; Schimel, J. P.; Palmer, R. G.; Hernandez-Viezcas, J. A.; Zhao, L.;
419 Gardea-Torresdey, J. L.; Holden, P. A., Soybean susceptibility to manufactured nanomaterials with
420 evidence for food quality and soil fertility interruption. *Proc. Natl. Acad. Sci. U. S. A.* **2012**, *109* (37),
421 E2451-E2456.
- 422 20. Lombi, E.; Nowack, B.; Baun, A.; McGrath, S. P., Evidence for effects of manufactured
423 nanomaterials on crops is inconclusive. *Proc. Natl. Acad. Sci. U. S. A.* **2012**, *109* (49), E3336.
- 424 21. Kopittke, P. M.; Menzies, N. W.; de Jonge, M. D.; McKenna, B. A.; Donner, E.; Webb, R. I.;
425 Paterson, D. J.; Howard, D. L.; Ryan, C. G.; Glover, C. J.; Scheckel, K. G.; Lombi, E., In situ
426 distribution and speciation of toxic copper, nickel, and zinc in hydrated roots of cowpea. *Plant*
427 *Physiol.* **2011**, *156* (2), 663-673.
- 428 22. Ravel, B.; Newville, M., ATHENA, ARTEMIS, HEPHAESTUS: data analysis for X-ray absorption
429 spectroscopy using IFEFFIT. *J. Synchrotron Radiat.* **2005**, *12*, 537-541.
- 430 23. Malinowski, E. R., *Factor analysis in chemistry*. John Wiley: New York, 1991.
- 431 24. Webb, S. M., SIXpack: A graphical user interface for XAS analysis using IFEFFIT. *Physica Scripta*
432 **2005**, *T115*, 1011-1014.
- 433 25. Wang, P.; Menzies, N. W.; Lombi, E.; McKenna, B. A.; de Jonge, M. D.; Donner, E.; Blamey, F. P.
434 C.; Ryan, C. G.; Paterson, D. J.; Howard, D. L.; James, S. A.; Kopittke, P. M., Quantitative

- determination of metal and metalloid spatial distribution in hydrated and fresh roots of cowpea using synchrotron-based X-ray fluorescence microscopy. *Sci. Total Environ.* **2013**, 463–464 (0), 131-139.
26. Ryan, C. G.; Etschmann, B. E.; Vogt, S.; Maser, J.; Harland, C. L.; van Achterbergh, E.; Legnini, D., Nuclear microprobe-synchrotron synergy: Towards integrated quantitative real-time elemental imaging using PIXE and SXRF. *Nucl. Instrum. Meth. B* **2005**, 231, 183-188.
27. Ryan, C. G.; Siddons, D. P.; Kirkham, R.; et al., The mew Maia detector system: Methods for high definition trace element imaging of natural material. In *X-Ray Optics and Microanalysis, Proceedings*, Denecke, M. A.; Walker, C. T., Eds. 2010; Vol. 1221, pp 9-17.
28. Donner, E.; Howard, D. L.; Jonge, M. D. d.; Paterson, D.; Cheah, M. H.; Naidu, R.; Lombi, E., X-ray absorption and micro X-ray fluorescence spectroscopy investigation of copper and zinc speciation in biosolids. *Environ. Sci. Technol.* **2011**, 45 (17), 7249-7257.
29. Hayes, S. M.; O'Day, P. A.; Webb, S. M.; Maier, R. M.; Chorover, J., Changes in zinc speciation with mine tailings acidification in a semiarid weathering environment. *Environ. Sci. Technol.* **2011**, 45 (17), 7166-7172.
30. Franklin, N. M.; Rogers, N. J.; Apte, S. C.; Batley, G. E.; Gadd, G. E.; Casey, P. S., Comparative toxicity of nanoparticulate ZnO, bulk ZnO, and ZnCl₂ to a freshwater microalga (*Pseudokirchneriella subcapitata*): The importance of particle solubility. *Environ. Sci. Technol.* **2007**, 41 (24), 8484-8490.
31. Miao, A. J.; Zhang, X. Y.; Luo, Z.; Chen, C. S.; Chin, W. C.; Santschi, P. H.; Quigg, A., Zinc oxide-engineered nanoparticles: dissolution and toxicity to marine phytoplankton. *Environ. Toxicol. Chem.* **2010**, 29 (12), 2814-2822.
32. Ma, H.; Williams, P. L.; Diamond, S. A., Ecotoxicity of manufactured ZnO nanoparticles – A review. *Environ. Pollut.* **2013**, 172 (0), 76-85.
33. Smolders, E.; Buekers, J.; Waegeneers, N.; Oliver, I.; McLaughlin, M. J. *Effects of field and laboratory Zn contamination on soil microbial processes and plant growth*; Katholieke Universiteit Leuven and Commonwealth Scientific and Industrial Research Organisation: Leuven, Belgium, 2003.
34. Zhao, L.; Hernandez-Viezcas, J. A.; Peralta-Videa, J. R.; Bandyopadhyay, S.; Peng, B.; Munoz, B.; Keller, A. A.; Gardea-Torresdey, J. L., ZnO nanoparticle fate in soil and zinc bioaccumulation in corn plants (*Zea mays*) influenced by alginate. *Environ. Sci. Proc. Impacts* **2013**, 15 (1), 260-266.
35. Waalewijn-Kool, P. L.; Diez Ortiz, M.; van Straalen, N. M.; van Gestel, C. A. M., Sorption, dissolution and pH determine the long-term equilibration and toxicity of coated and uncoated ZnO nanoparticles in soil. *Environ. Pollut.* **2013**, 178 (0), 59-64.
36. Collins, D.; Luxton, T.; Kumar, N.; Shah, S.; Walker, V. K.; Shah, V., Assessing the impact of copper and zinc oxide nanoparticles on soil: A field study. *PLoS One* **2012**, 7 (8), e42663.
37. Gimbert, L. J.; Hamon, R. E.; Casey, P. S.; Worsfold, P. J., Partitioning and stability of engineered ZnO nanoparticles in soil suspensions using flow field-flow fractionation. *Environ. Chem.* **2007**, 4 (1), 8-10.

- 471 38. Salt, D. E.; Prince, R. C.; Baker, A. J. M.; Raskin, I.; Pickering, I. J., Zinc ligands in the metal
472 hyperaccumulator *Thlaspi caerulescens* as determined using X-ray absorption spectroscopy. *Environ.*
473 *Sci. Technol.* **1999**, *33* (5), 713-717.
- 474 39. Kupper, H.; Lombi, E.; Zhao, F. J.; McGrath, S. P., Cellular compartmentation of cadmium and zinc
475 in relation to other elements in the hyperaccumulator *Arabidopsis halleri*. *Planta* **2000**, *212* (1), 75-
476 84.
- 477 40. Zhao, F. J.; Lombi, E.; Breedon, T.; McGrath, S. P., Zinc hyperaccumulation and cellular distribution
478 in *Arabidopsis halleri*. *Plant Cell Environ.* **2000**, *23* (5), 507-514.
- 479 41. Sarret, G.; Saumitou-Laprade, P.; Bert, V.; Proux, O.; Hazemann, J. L.; Traverse, A. S.; Marcus, M.
480 A.; Manceau, A., Forms of zinc accumulated in the hyperaccumulator *Arabidopsis halleri*. *Plant*
481 *Physiol.* **2002**, *130* (4), 1815-1826.
- 482 42. Ryan, C. A.; Walkersimmons, M., Plant vacuoles. *Methods in Enzymology* **1983**, *96*, 580-589.
- 483 43. Sarret, G.; Willems, G.; Isaure, M. P.; Marcus, M. A.; Fakra, S. C.; Frerot, H.; Pairis, S.; Geoffroy,
484 N.; Manceau, A.; Saumitou-Laprade, P., Zinc distribution and speciation in *Arabidopsis halleri* x
485 *Arabidopsis lyrata* progenies presenting various zinc accumulation capacities. *New Phytol.* **2009**, *184*
486 (3), 581-595.
- 487 44. Raboy, V., myo-Inositol-1,2,3,4,5,6-hexakisphosphate. *Phytochemistry* **2003**, *64* (6), 1033-1043.
- 488 45. Vasca, E.; Materazzi, S.; Caruso, T.; Milano, O.; Fontanella, C.; Manfredi, C., Complex formation
489 between phytic acid and divalent metal ions: a solution equilibria and solid state investigation. *Anal.*
490 *Bioanal. Chem.* **2002**, *374* (1), 173-178.
- 491 46. Mills, E. N. C.; Parker, M. L.; Wellner, N.; Toole, G.; Feeney, K.; Shewry, P. R., Chemical imaging:
492 the distribution of ions and molecules in developing and mature wheat grain. *J. Cereal Sci.* **2005**, *41*
493 (2), 193-201.
- 494 47. Persson, D. P.; Hansen, T. H.; Laursen, K. H.; Schjoerring, J. K.; Husted, S., Simultaneous iron, zinc,
495 sulfur and phosphorus speciation analysis of barley grain tissues using SEC-ICP-MS and IP-ICP-MS.
496 *Metallomics* **2009**, *1* (5), 418-426.
- 497 48. Hatzack, F.; Johansen, K. S.; Rasmussen, S. K., Nutritionally relevant parameters in low-phytate
498 barley (*Hordeum vulgare* L.) grain mutants. *J. Agr. Food Chem.* **2000**, *48* (12), 6074-6080.
- 499 49. Kirpichtchikova, T. A.; Manceau, A.; Spadini, L.; Panfili, F.; Marcus, M. A.; Jacquet, T., Speciation
500 and solubility of heavy metals in contaminated soil using X-ray microfluorescence, EXAFS
501 spectroscopy, chemical extraction, and thermodynamic modeling. *Geochim. Cosmochim. Ac.* **2006**,
502 *70* (9), 2163-2190.
- 503 50. Manceau, A.; Marcus, M. A.; Tamura, N., Quantitative speciation of heavy metals in soils and
504 sediments by synchrotron X-ray techniques. *Rev. Mineral. Geochem.* **2002**, *49* (1), 341-428.

Table 1. Distributions of Zn species in various tissues of cowpea grown in either solution culture or soil culture^a

	Nodule		Root		Stem		Leaf		Seed	
	ZnO-NP	ZnCl ₂	ZnO-NP	ZnCl ₂	ZnO-NP	ZnCl ₂	ZnO-NP	ZnCl ₂	ZnO-NP	ZnCl ₂
Solution culture										
ZnO-NPs (%)			65 (1.1)							
Zn-PGA (%) ^c				32 (0.7)						
Zn-citrate (%)					76 (0.6)	63 (1.0)	60 (1.2)	75 (1.0)		
Zn-histidine (%)			32 (0.9)	49 (1.7)	14 (1.0)	17 (1.5)	25 (1.9)	10 (1.5)		
Zn-phytate (%)					10 (1.2)	20 (2.0)	15 (2.4)	15 (1.9)		
Zn-cysteine (%)										
Zn-phosphate (%)			3 (0.7)	19 (3.0)						
R-factor ^b			0.0001	0.0002	0.0001	0.0003	0.0005	0.0003		
Soil culture										
Zn-citrate (%)	42 (1.5)	31 (1.2)	59 (0.8)	43 (0.8)	27 (1.1)	34 (1.9)	50 (0.9)	41 (0.7)		
Zn-histidine (%)			25 (1.2)	30 (1.2)	38 (1.6)	34 (2.9)	43 (1.4)	27 (1.1)	56 (1.3)	45 (1.4)
Zn-phytate (%)	38 (2.1)	37 (1.4)	16 (1.4)	27 (1.5)	35 (2.1)	32 (3.6)	7 (1.8)	32 (1.4)		
Zn-cysteine (%)	22 (0.9)	32 (0.7)							24 (1.1)	36 (1.1)
Zn-phosphate (%)									20 (1.7)	19 (1.8)
R-factor ^b	0.0006	0.0003	0.0002	0.0002	0.0004	0.0005	0.0003	0.0002	0.0003	0.0004

^aData are presented as percentages and the values in brackets show the percentage variation in the calculated values. ^bR factor = $\sum(\text{experimental} - \text{fit})^2 / \sum(\text{experimental})^2$, where the sums are over the data points in the fitting region. ^cPGA: polygalacturonic acid.

Table 2. Best fit speciation of Zn in soils as identified by linear combination fitting (LCF) of K_{α} -edge XANES and EXAFS spectra^a

	XANES				EXAFS				
	ZnAl-LDH	Zn-sorb ferr. ^c	ZnSO ₄	R-factor ^b	ZnAl-LDH	hemimorphite	ZnSO ₄	R-factor ^b	
Oxisol									
ZnO-NPs 1h	30 (1.0)	45 (0.6)	25 (1.2)	0.0003	38 (5.2)	44 (1.6)	18 (5.5)	0.057	
ZnO-NPs 1d	24 (1.1)	44 (0.6)	32 (1.2)	0.0003	26 (5.4)	48 (1.6)	26 (5.6)	0.063	
ZnO-NPs 5d	28 (1.1)	41 (0.6)	31 (1.3)	0.0004	36 (5.1)	41 (1.5)	23 (5.3)	0.057	
ZnO-NPs 15d	24 (1.2)	43 (0.7)	33 (1.4)	0.0004	27 (5.4)	45 (1.7)	28 (5.7)	0.066	
ZnCl ₂ 1 h	23 (1.5)	55 (0.8)	22 (1.7)	0.0007	24 (5.5)	47 (1.7)	29 (5.7)	0.081	
ZnCl ₂ 1 d	22 (1.4)	53 (0.8)	25 (1.6)	0.0005	29 (5.7)	47 (1.7)	24 (5.9)	0.082	
ZnCl ₂ 5 d	21 (1.6)	55 (0.9)	24 (1.8)	0.0004	22 (6.9)	53 (2.1)	25 (7.2)	0.096	
ZnCl ₂ 15 d	22 (1.4)	54 (0.8)	24 (1.6)	0.0006	22 (5.9)	45 (1.8)	33 (6.1)	0.088	
	ZnAl-LDH	HA-Zn	hopeite	ZnSO ₄					
Ultisol									
ZnO-NPs 1h	15 (0.7)	29 (1.8)	17 (1.4)	40 (2.3)	0.0001	31 (6.5)	36 (2.0)	33 (6.7)	0.079
ZnO-NPs 1d	16 (0.8)	27 (1.8)	16 (1.4)	41 (2.4)	0.0001	31 (6.3)	35 (1.9)	34 (6.6)	0.076
ZnO-NPs 5d	12 (0.9)	27 (2.2)	15 (1.7)	46 (2.9)	0.0002	36 (5.1)	41 (1.5)	23 (5.3)	0.058
ZnO-NPs 15d	9 (0.9)	28 (2.2)	15 (1.7)	49 (2.9)	0.0002	27 (5.4)	45 (1.7)	28 (5.7)	0.066
ZnCl ₂ 1 h	10 (0.9)	21 (2.1)	19 (1.7)	50 (2.9)	0.0002	26 (7.5)	32 (2.3)	42 (7.8)	0.097
ZnCl ₂ 1 d	13 (1.1)	10 (0.8)	26 (2.0)	51 (3.5)	0.0002	18 (6.5)	35 (2.0)	47 (6.8)	0.080
ZnCl ₂ 5 d	16 (1.1)	24 (2.4)	50 (1.9)	10 (3.3)	0.0002	34 (7.2)	46 (2.2)	20 (7.6)	0.109
ZnCl ₂ 15 d	16 (1.2)	27 (2.6)	47 (2.0)	10 (3.5)	0.0003	32 (8.4)	45 (2.6)	23 (8.8)	0.140

^aData are presented as percentages and the values in brackets show the percentage variation in the calculated values. ^bR factor = $\sum(\text{experimental} - \text{fit})^2 / \sum(\text{experimental})^2$, where the sums are over the data points in the fitting region. ^cZn sorbed ferrihydrite.

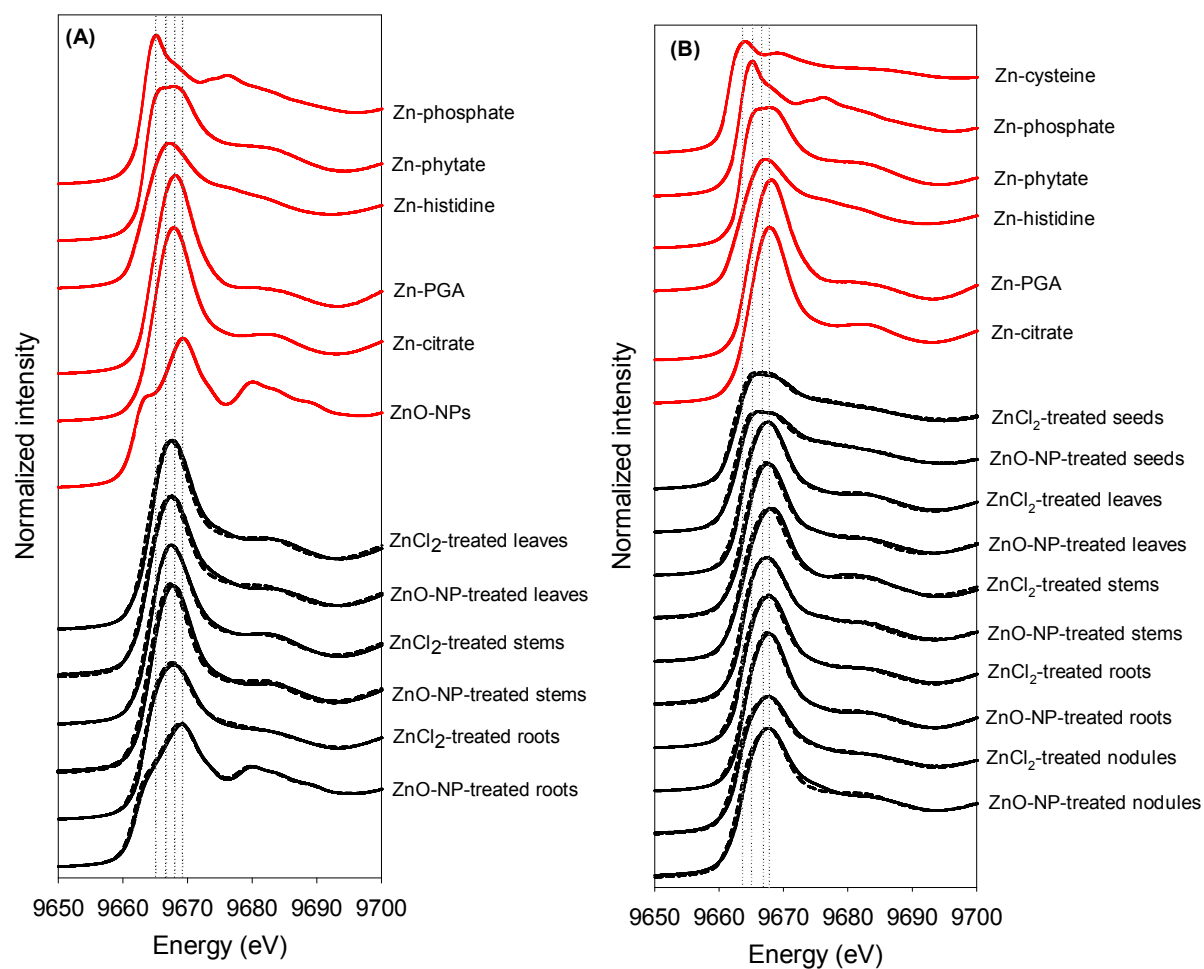


Figure 1. Normalized Zn K_{α} -edge XANES spectra for various tissues of cowpea exposed to ZnO-NPs or ZnCl₂ in solution culture (A) or soil culture (B). Data are also presented for the standard compounds determined in the LCF solutions. Dotted lines show the best fits of reference spectra obtained using LCF as presented in Table 1.

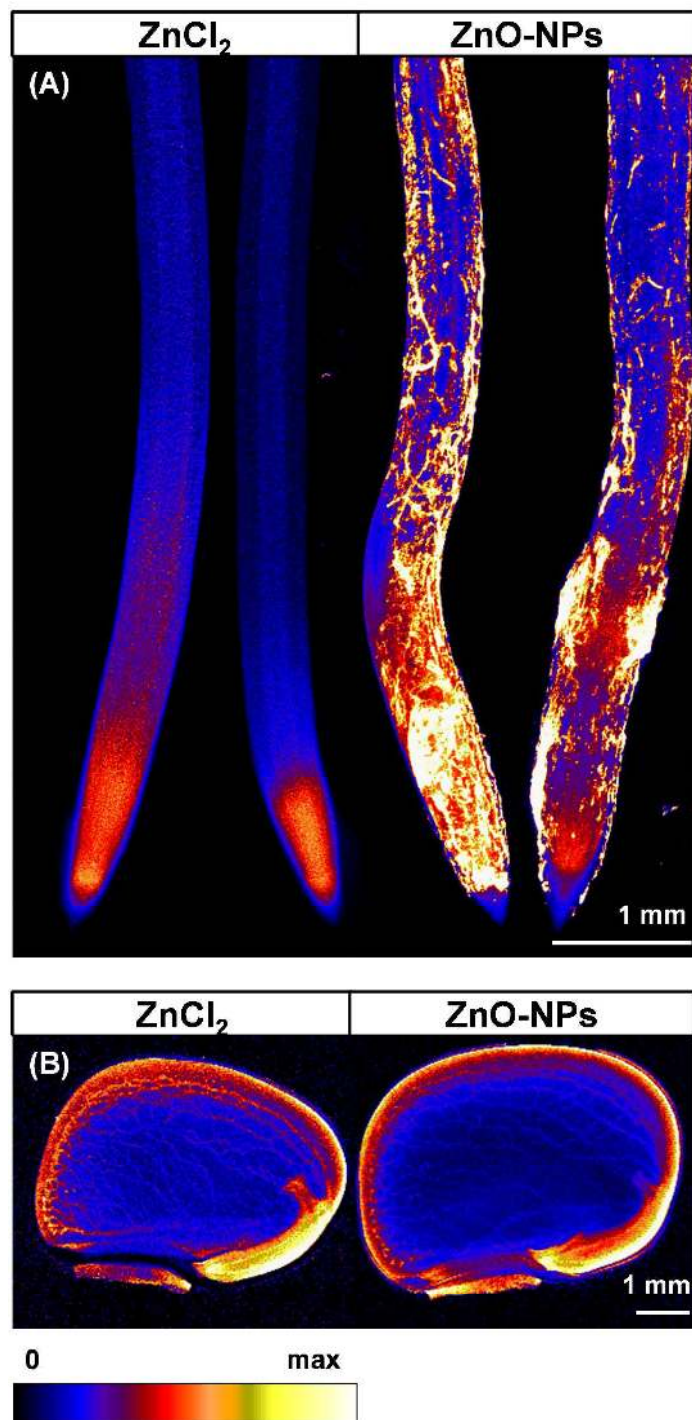


Figure 2. (A) Imaging of Zn in cowpea roots exposed for 1 d to 25 mg Zn L^{-1} as ZnO-NPs or ZnCl_2 in solution culture using $\mu\text{-XRF}$. (B) Imaging of Zn in cowpea seeds grown in the Oxisol amended with ZnCl_2 or ZnO-NPs using $\mu\text{-XRF}$. All samples were enclosed in $4 \mu\text{m}$ -thick Ultralene films and scanned simultaneously allowing valid comparisons between treatments. Brighter colors correspond to higher Zn concentrations.

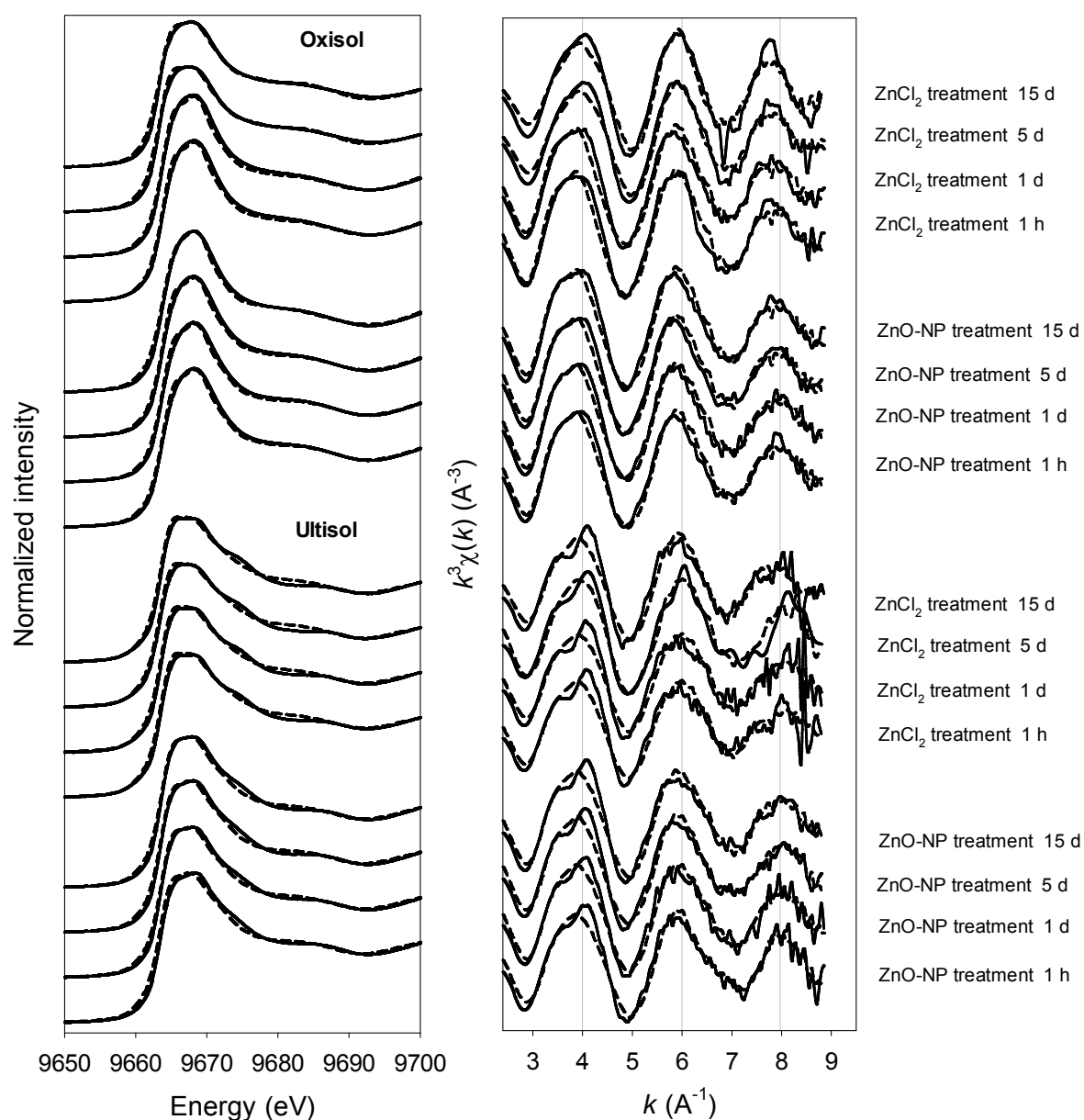
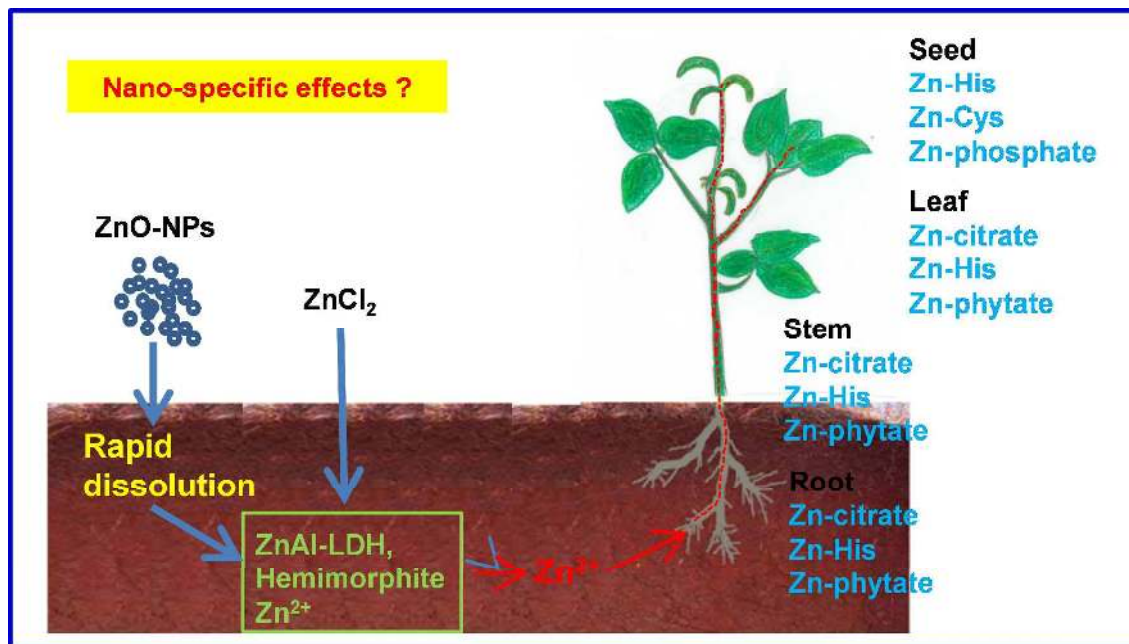


Figure 3. Zn K_{α} -edge XANES and k^3 -weighted EXAFS spectra of two soils (Oxisol and Ultisol) amended with 500 mg Zn kg⁻¹ as ZnCl₂ or ZnO-NPs incubated for 1 h, 1 d, 5 d, and 15 d. Dotted lines show the best fits of reference spectra obtained using LCF as presented in Table 2.



TOC Graphic Image